EXCITATION OF ELECTRON PLASMA WAVE BY SELF FOCUSED COSH-GAUSSIAN LASER BEAMS IN COLLISIONLESS PLASMAS: EFFECT OF DENSITY RAMP **

Naveen Gupta [1], Sanjeev Kumar [2], S. B. Bhardwaj [3*]

[1] Department of Physics, Lovely Professional University, Phagwara, India
[2] Department of Physics, Government College for Women, Karnal, India
[3] Department of Physics, SUS Govt. College, Matak-Majri, Karnal, India;
e-mail: naveens222@rediffmail.com

Dynamics of the laser driven electron plasma waves (EPWs) in plasmas with axial density ramp has been investigated theoretically. The effect of self-focusing of the laser beam on the power of laser excited EPW has been incorporated. During its propagation through the plasma, the laser beam excites an EPW at frequency ω_{ep} that due to the optical nonlinearity of plasma gets nonlinearly coupled to the laser beam. Using variational theory semi analytical solutions of the coupled nonlinear wave equations for the pump wave and EPW have been obtained under W.K.B. approximation technique. It has been observed that power of the EPW is significantly affected by the self-focusing effect of pump beam.

Keywords: *self-focusing, electron plasma wave, cosh-Gaussian, ponderomotive force.*

ВОЗБУЖДЕНИЕ ЭЛЕКТРОННОЙ ПЛАЗМЕННОЙ ВОЛНЫ САМОФОКУСИРУЮЩИМИСЯ COSH-ГАУССОВЫМИ ЛАЗЕРНЫМИ ПУЧКАМИ В НЕОДНОРОДНОЙ БЕССТОЛКНОВИТЕЛЬНОЙ ПЛАЗМЕ

N. Gupta [1], Sanjeev Kumar [2], S. B. Bhardwaj [3*]

УДК 535.375.5;621.375.826

[1] Университет Пхагвара, Пхагвар, Индия
[2] Государственный колледж для женщин, Карнал, Индия
[3] Государственный колледж SUS, Матак-Маджри, Карнал, Индия;
e-mail: naveens222@rediffmail.com

(Поступила 23 марта 2022)

Теоретически исследована динамика управляемых лазером волн электронной плазмы (EPW) в плазме с осевым скачком плотности с учетом самофокусировки лазерного луча на мощность EPW, возбуждаемого лазером. Во время распространения через плазму лазерный луч возбуждает EPW с частотой ω_{ep}, которая из-за оптической нелинейности плазмы нелинейно связана с лазерным лучом. На основе вариационной теории получены полуаналитические решения связанных нелинейных волновых уравнений для волны накачки и EPW с использованием квазиклассического приближения. Показано, что на мощность EPW существенно влияет эффект самофокусировки луча накачки.

Ключевые слова: *самофокусировка, электронно-плазменная волна, cosh-гауссов лазерный пучок, пондеромоторная сила.*

Introduction. Investigations on coupling of intense laser beams with plasmas is at the vanguard of research since past few decades due to its importance in many potential applications including laser fusion [1–3], plasma wake field accelerators [4, 5], X-ray lasers [6, 7], terahertz generation [8] etc. The ultimate breath of these applications depends on the efficiency of laser plasma coupling which is further decided by

**Full text is published in JAS V. 90, No. 1 (http://springer.com/journal/10812) and in electronic version of ZhPS V. 90, No. 1 (http://www.elibrary.ru/title_about.asp?id=7318; sales@elibrary.ru).

many different nonlinear processes [9–11]. These processes range from collisional absorption to excitation of copious laser driven instabilities [12–15]. These instabilities can be represented as the resonant coupling of the incident laser beam into two daughter waves. In the absence of external magnetic field these daughter waves can be electron plasma waves, ion acoustic waves along with a scattered electromagnetic wave.

Electron plasma waves (EPWs) can be excited in plasmas due to their remarkable properties of quasi neutrality and collective behaviour. Plasma is a state of matter that contains enough heat that atoms lose their individuality. The negatively charged electrons are still attracted by positively charged nuclei, but they are not bound together. This gives a plasma some unusual properties unlike most kind of ordinary matter-solids, liquids and gases-the free-floating electrons and ions of a plasma are strongly affected by electric and magnetic fields. Plasma as a whole is quasi neutral, but as the electrons and positively charged ions are separated, a disturbance can create regions of net negative and net positive charges acting like the plates of a charged parallel plate capacitor. Such an uneven distribution of charges results in an electric field running from positive to negative regions. This electric field pulls the electrons and ions towards each other with equal forces. Due to their large mass ions are lazy and thus remain at rest and the electrons move towards the ions. As the electrons move towards the ions, they steadily gain velocity and momentum like a pendulum moving towards its mean position from an extreme position. Due to this gain in momentum the electrons overshoot their equilibrium positions resulting in reversing the direction of electric field. Now the reversed electric field opposes the electron motion slow them down and then pulling them back again. The process repeats itself, establishing an electron oscillator. In the presence of thermal velocity these electron oscillations lead to a longitudinal wave compression and rarefaction regions of electrons propagating through the plasma known as EPW.

The excited EPW through SRS is having very high phase velocity and therefore can lead to the generation of super thermal electrons in inertial confinement fusion (ICF). These penetrating electrons can preheat the fuel and prevent the efficient compression required for high gain [16]. When a super thermal electron escapes from the pellet, it leaves a net positive charge on the pellet. This positive charge attracts the outward moving super thermal electron back towards the pellet, where upon they overshoot their original position and pose on into the pellet core. Some of the most energetic electrons may oscillate several times through the pellet before collisions with the fuel finally slow them. The transfer of collisional energy to the fuel preheats the pellet. The phenomenon is referred to as preheating [17].

The attractive electrostatic force between the supra thermal electrons and the ions in the corona can also lead to the outward acceleration of highly energetic ions. The loss of energetic ions from the ablation layer also drains way laser energy that might otherwise drive the implosion.

The super thermal electrons may also have such a long range that collisions with “colder” electrons become less frequent, so that the rate of heat transfer between the atmosphere and the pellet drops and the pellet fails to implode properly. This is called decoupling [18]. Thus, in order to achieve successful ignition of the target it becomes vital to investigate SRS of intense laser beams in plasmas.

Most laser beams have a Gaussian irradiance profile, although it can be beneficial to use a non-Gaussian beam in certain applications. The irradiance cross-section of Gaussian beams decreases symmetrically with increasing distance from the center; in contrast, flat-top beams, also known as top-hat beams, maintain a constant irradiance value through a beam cross-section, providing a consistent intensity across the target of a laser system [19, 20]. This results in more accurate and predictable results in applications such as semiconductor wafer processing, other materials processing, and nonlinear frequency conversion with high-power beams. Compared to Gaussian beams, flat-top beams can generate cleaner cuts and sharper edges in processing systems. Gaussian laser profiles have several disadvantages, such as the low-intensity portions on either side of the usable central region of the beam, known as “wings.” These wings typically contain energy that is wasted because it is at a lower intensity than the threshold required for the given application, whether it is materials processing, laser surgery, laser driven fusion or another application where an intensity above a given value is needed. The wings of a Gaussian beam may also damage surrounding areas outside of the target area, extending the heat-affected zone. This is unfavourable in situations like laser surgery and precise materials processing where high accuracy and minimized damage to surrounding areas are prioritized. Features formed using a Gaussian beam won’t have particularly smooth edges because of this effect, which reduces system accuracy.

The lack of wings and steeper edge transitions in flat-top beam profiles result in more efficient energy delivery compared to Gaussian beams, as well as smaller heat affected zones. Any features etched, welded, or cut using a flat-top beam will be more accurate and there will be less damage to surrounding areas. The

well-defined and consistent irradiance profile of flat-top beams minimizes both measurement uncertainty and statistical variance. Flat-top beams are also advantageous in many fluorescence microscopy, holography, and interferometry systems. Such laser beams are modelled by super Gaussian profile. However, super Gaussian irradiance profile is an ideal concept. Experimentally the laser beams with uniform irradiance over their cross section can be produced by superposition of multiple decentered Gaussian laser beams. One such beam profile is modelled by cosh-Gaussian (ChG) irradiance profile [21, 22]. Literature review reveals the fact that most of the earlier investigations on excitation of EPWs by intense laser beams in plasmas have been reported for Gaussian laser beams. Thus, this article aims to give first theoretical investigation on EPW excitation by ChG laser beams in plasma with axial density ramp by incorporating the effect of self-focusing.

Characteristics of cosh-Gaussian laser beam. The amplitude structure over the cross section of ChG laser beam is given [22]:

$$E_0\left(r, z=0\right) = E_{00}\exp\left(-\frac{r^2}{2r_0^2}\right)\cosh\left(b\frac{r}{r_0}\right), \tag{1}$$

where, E_{00} is the axial amplitude of the laser beam and r_0 is the spot size of the laser beam at the plane of incidence i.e., $z = 0$. The parameter b associated with the Cosh function is known as Cosh factor. It is the key parameter of interest because it acts as a control parameter to control the dynamics of the pump beam and hence the beam scattered through the SRS process. Eq. (1) can also be written as

$$E_0\left(r,z=0\right) = \frac{E_{00}}{2}\exp(b^2/2)\left[e^{-\left(\frac{r}{r_0}-b\right)^2} + e^{-\left(\frac{r}{r_0}+b\right)^2} + 2e^{-\left(\frac{r^2}{r_0^2}+b^2\right)}\right]^{1/2}.$$

From this equation it can be seen that ChG laser beams can be realized experimentally by the in phase superposition of two otherwise identical Gaussian beams whose intensity maxima instead of lying at beam axes lie at coordinates $\left(\pm\frac{b}{2}r_0\ ,0\right)$, respectively. Thus, the factor b is associated with the displacement of the intensity maxima of the constituting beams from their axis and hence it is also known as decentered parameter. In order to see the effect of the cosh factor 'b' on the irradiance over the cross section of the laser beam we have portrayed the initial irradiance profile (variation of intensity of the laser beam with transverse directions) of the laser beam in Fig. 1 for different values of b.

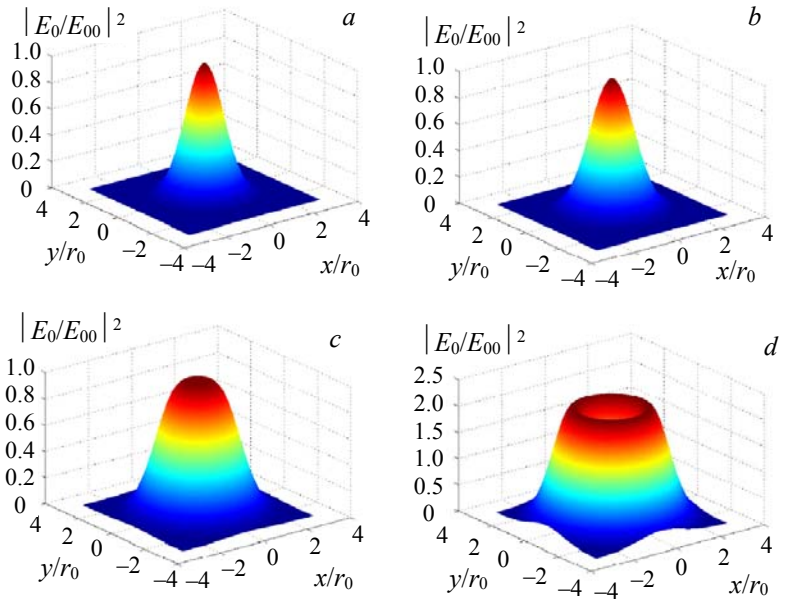

Fig. 1. 3D intensity plots of ChG laser beam for b = 0 (a), 0.5 (b), 1 (c), and 1.45 (d).

It can be seen that for small values of b the irradiance over the cross section of the laser beam is similar to Gaussian profile. However, as the value of b increases for $0 \le b \le 1$ the intensity profile start getting flatter and the degree of flatness increases with increase in the value of b. It can also be seen that as the value of b becomes greater than 1, a central dip appear in the intensity profile i.e., for $b > 1$ the intensity profile of ChG laser beam consists of a central dark disk surrounded by a bright ring.

For $z > 0$ the energy conserving ansatz for the ChG laser beam is given by

$$E_0(r,z) = \frac{E_{00}}{f}\exp\left(-\frac{r^2}{2r_0^2 f^2}\right)\cosh\left(\frac{b}{r_0 f}r\right). \tag{2}$$

Here, the function $f(z)$ is currently undetermined parameter and is termed as a dimensionless beam width parameter. Its significance is twofold: (1) upon multiplication with equilibrium beam width r_0 it gives the instantaneous spot size of the beam at a given location inside the medium; (2) upon division with amplitude it gives the measure of instantaneous intensity of the beam.

Optical nonlinearity of plasma. Consider the propagation of a laser beam with electric field vector

$$\mathbf{E}(r,t) = E_0(r,z)e^{-i(k_0 z-\omega_0 t)}\mathbf{e}_x \tag{3}$$

through a collisionless plasma whose equilibrium electron density (i.e., the density in the absence of laser beam) is having a upward ramp shaped profile modelled by

$$n_0(z) = n_0^0\left(1+\tan(dz)\right). \tag{4}$$

Here, n_0^0 is the electron density at $z = 0$ i.e., the density at the plane of incidence and the constant d gives the measure of rate of increase of electron density with distance. Hence the parameter d is termed as slope of the ramp; k_0, ω_0 are the wavenumber and angular frequency of the laser beam, respectively.

The nonuniform amplitude structure over the cross section of the laser beam given by Eq. (2), results in a transverse force known as ponderomotive force $\left(F_p = -\frac{e^2}{4m\omega_0^2}\nabla\left(E_0E_0^\star\right)\right)$ acting on the plasma electrons. Due to this force the plasma electrons start migrating from high intensity regions of the illuminated portion of plasma towards the low intensity regions.

The resulting electron density of plasma is given by

$$n(r,z) = n_0(z)\exp\left[-\frac{e^2}{8m\omega_0^2 T_0 K_0}E_0E_0^\star\right], \tag{5}$$

where, T_0 is the temperature of plasma electrons and K_0 is the Boltzmann constant. The modified electron density in turn alters the dielectric function $\left(\varepsilon = 1-\frac{4\pi e^2 n}{m\omega_0^2}\right)$ of plasma:

$$\varepsilon = 1-\frac{\omega_{p0}^2}{\omega_0^2}\left(1+\tan(dz)\right)\exp\left[-\frac{e^2}{8m\omega_0^2 T_0 K_0}E_0E_0^\star\right]. \tag{6}$$

Here, $\left(\omega_{p0}^2 = \frac{4\pi e^2}{m}n_0^0\right)$ corresponds to the unperturbed plasma frequency i.e., plasma frequency in the absence of laser beam. Thus, the ponderomotive force on the plasma electrons produced by the laser beam, makes the index of refraction of plasma intensity dependent which in turn due to spatial dependence of the amplitude structure of the laser beam, resembles to that of graded index fiber. Separating the dielectric function of plasma into linear ε_0 and nonlinear $\phi\left(E_0E_0^\star\right)$ parts as $\varepsilon = \varepsilon_0 + \phi\left(E_0E_0^\star\right)$

$$\varepsilon_0 = 1-\omega_{p0}^2/\omega_0^2, \tag{7}$$

$$\phi\left(E_0E_0^\star\right) = \omega_{p0}^2/\omega_0^2\left\{1-\left(1+\tan(dz)\right)\exp\left[-\frac{e^2}{8m\omega_0^2 T_0 K_0}E_0E_0^\star\right]\right\}. \tag{8}$$

Evolution of beam envelope. The model equation governing the evolution of a laser beam through a nonlinear medium characterized by dielectric function of the form given by Eq. (8):

$$2ik_0\frac{\partial E_0}{\partial z}=\nabla_\perp^2 E_0+\frac{\omega_0^2}{c^2}\phi\left(E_0E_0^\star\right)E_0\ . \tag{9}$$

Eq. (9) is the well-known nonlinear Schrodinger wave equation (NSWE) as its mathematical structure is very much similar to the Schrodinger wave equation of quantum mechanics. Due to the presence of nonlinear term $\phi\left(E_0E_0^\star\right)$, Eq. (9) does not possess any exact analytic solution. The only way to get physical insight into the propagation dynamics of the laser beam is to solve Eq. (9) either by some numerical method or by semi analytic method. For partial differential equations the numerical methods however, are very time consuming and suffer from serious convergence problems. Hence, in the present analysis we have used a semi analytical technique known as variational method [23, 24]. This method allows one to obtain approximate solution of Eq. (9) by converting it to a set of coupled differential equations for the parameters of interest. According to this method Eq. (9) is a variational problem for action principle based on lagrangian density

$$\mathcal{L}=i\left(E_0\frac{\partial E_0^\star}{\partial z}-E_0^\star\frac{\partial E_0}{\partial z}\right)+\left|\nabla_\perp E_0\right|^2-\frac{\omega_0^2}{c^2}\int\phi\left(E_0E_0^\star\right)d\left(E_0E_0^\star\right). \tag{10}$$

Substituting the trial function given by Eq. (2) in lagrangian density and integrating over the entire cross section of the laser beam, we get the reduced lagrangian as $L=\int\mathcal{L}\left(E_0,E_0^\star,\phi\right)d^2r$.

The corresponding Euler Lagrange equation

$$\frac{d}{dz}\left(\frac{\partial L}{\partial\left(\partial f/\partial z\right)}\right)-\partial L/\partial f=0 \tag{11}$$

gives the differential equation for the evolution of beam width of the laser beam:

$$\frac{d^2f}{d\xi^2}=\left(\frac{1+e^{-b^2}\left(1-b^2\right)}{2\left(1+b^2\right)}\right)\frac{1}{f^3}-\left(\frac{e^{-b^2}}{1+b^2}\right)\left(\frac{\omega_{p0}^2c^2}{c^2}\right)\frac{\beta E_{00}^2}{f^3}\left(1+\tan\left(d'\xi\right)\right)\left(T_1-bT_2\right), \tag{12}$$

where,

$$T_1=\int_0^\infty x^3e^{-2x^2}\cosh^4\left(bx\right)\exp\left[-\frac{\beta E_{00}^2}{f^2}e^{-x^2}\cosh^2\left(bx\right)\right]dx,$$

$$T_2=\int_0^\infty x^2e^{-2x^2}\cosh^3\left(bx\right)\sinh\left(bx\right)\exp\left[-\frac{\beta E_{00}^2}{f^2}e^{-x^2}\cosh^2\left(bx\right)\right]dx,$$

$$x=r/r_0f\ ,\quad \xi=z/k_0r_0^2.$$

Equation (12) governs the evolution of beam width of ChG laser beam along the distance of propagation through plasma. For initially collimated laser beam (i.e., laser beam having a plane wavefront) Eq. (12) is subjected to initial conditions $f(0)=1$ and $\frac{df}{d\xi}\Big|_{\xi=0}=0$. In present investigation Eq. (12) has been solved numerically for the following set of laser and plasma parameters $\omega_0=1.78\times10^{15}\,\text{rad/s};\ r_0=15\mu\text{m};\beta E_{00}^2=3;\left(\omega_{p0}r_0/c\right)^2=9;T_0=10^6\,\text{K}$ and for different values of Cosh factor and the slope of density ramp i.e., b = (0, 0.5, 1.0, 1.1, 1.2, 1.3) and d' = (0.025, 0.035, 0.045) and the corresponding evolutions of beam width of the laser beam have been shown in Figs. 2 and 3. It can be seen that during the propagation of the laser beam through plasma its spot size shows harmonic variations over the distance of propagation. This behaviour of the laser beam can be explained by identifying the physical significance of various terms contained in Eq. (12). The first term on the right-hand side that varies inversely as the cube of the beam width models the diffraction broadening of the laser beam. It indicates that smaller is the beam width larger will be the diffraction broadening of the laser beam. This is due to the fact that a laser beam with finite cross section can be considered as a superposition of plane waves, all having the same wave number, but with different angle with respect to the beam axis. Therefore, each component propagates at different phase velocity with respect to the longitudinal direction. Thus, each plane wave acquires a different phase and thus the beam broadens along the transverse directions. The components closer to the beam axis

make larger angles with the beam axis and thus broaden more. Smaller will be the spot size of the laser beam, larger will be the number of plane wave components closer to the beam axis. Hence, laser beams with smaller spot size broaden more.

The second term on the right-hand side of Eq. (12) originates due to the ponderomotive force acting on the plasma electrons that causes the evacuation of plasma electrons from the beam axis towards its tail i.e., the beam digs a density channel into the plasma. In case of plasma lesser is the electron density more is the index of refraction. Thus, the axial part of the laser beam experience higher index of refraction compared its wings. The resulting gradient in the phase velocity of the laser beam along its cross section, results in the inward bending of its phase fronts as if the beam is passing through a convex lens. This phenomenon is known as self-focusing because the beam gets focused by its own without requiring any lens structure. As this phenomenon occurs due to the intensity dependence of the index of refraction, the second term on the right-hand side of Eq. (12) is known as nonlinear refractive term.

Thus, two separate physical phenomena account for the propagation of high-power laser light through plasmas: (1) nonlinear refraction and (2) diffraction broadening. The winning phenomenon decides whether the beam will diverge of converge. Thus, there exists a threshold beam intensity above which the beam will converge due to self-focusing. The value of this threshold intensity can be obtained by equating the right-hand side of Eq. (12) with zero. In the present investigation we have taken the initial intensity of the laser beam to be greater than the threshold intensity for self-focusing, that is why the laser beam starts converging immediately after its entry into the plasma. With the decrease in the spot size of the laser beam its peak intensity start increasing resulting in more depletion of electron density from the illuminated portion of plasma. When the intensity of the laser beam becomes too high, the illuminated portion of plasma becomes almost evacuated from electrons. Now the laser beam propagates as if it is propagating through vacuum. Hence, after attaining minimum possible value, the beam width of the laser beam bounces back towards its original value. As the beam width of the laser beam starts increasing, the competition between nonlinear refraction and diffraction starts again. Now this competition lasts till the beam width of the laser beam attains its maximum possible value. These processes keep on repeating themselves and give a oscillatory character to the beam width of the laser beam.

Further it has been observed that after every focal spot the maximum as well as the minimum of the beam width shift downwards. This is owing to the fact that the equilibrium electron density is an increasing function of longitudinal distance. Hence, the plasma index of refraction keeps on decreasing with the penetration of laser beam into the plasma. Consequently, the self-focusing effect gets enhanced and the maximum as well as minimum of the beam width go on shifting downwards after every focal spot. It is also seen that the frequency of oscillations of beam with increases with distance. The physics behind this fact is that denser is the plasma, higher will be the phase velocity of laser beam through it. Hence, in denser plasma laser beam takes less duration to get self-focused.

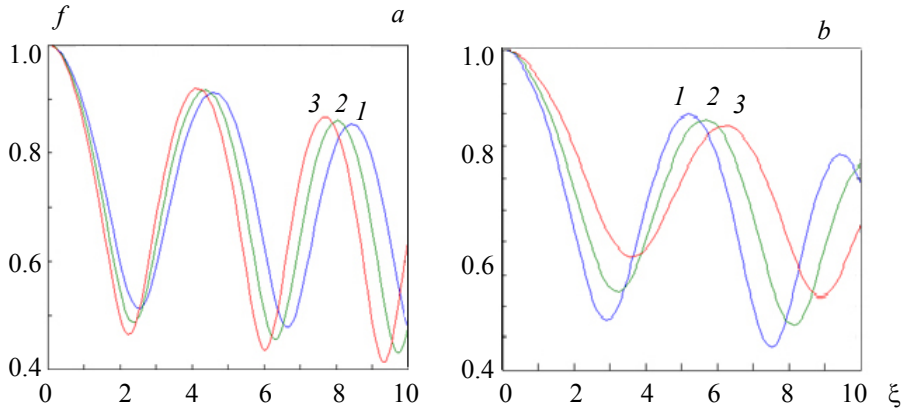

Fig. 2. Effect of the Cosh factor on the evolution of the beam width of the laser beam through plasma for a fixed value of the slope of the density ramp $d' = 0.025$: a) $b = 0$ (*1*), 0.5 (*2*), and 1.0 (*3*), b) $b = 1.1$ (*1*), 1.2 (*2*), and 1.3 (*3*).

Figure 2 depicts the effect of the Cosh factor b on the extent of self-focusing of the laser beam. It can be seen that for $0 \le b \le 1$ with an increase of b, the extent of self-focusing increases, whereas the scenario gets reversed after $b > 1$, i.e., for $b > 1$ with an increase in the value of b the extent of self-focusing of the laser beam gets reduced. This is due to the fact that for $0 \le b \le 1$ with an increase in the value of b, the uniformity of the irradiance over the cross section of the laser beam increases. Hence, the laser beam gets equal contribution from off axial rays to the nonlinear refraction. As the nonlinear refraction of the laser beam is homeostasis for its self-focusing, with an increase in the value of b, for $0 \le b \le 1$, the extent of self-focusing of the laser beam increases. However, for $b > 1$ due to the presence of the central dark region, the ChG laser beam does not get any contribution from the axial part of the wave fronts to the nonlinear refraction. Since, the area of the central dark region increases with an increase in the value of b for $b>1$, the extent of self-focusing starts decreasing with an increase in the value of the Cosh factor for $b>1$. Figure 2 depicts the effect of Cosh factor b on the extent of self-focusing of the laser beam. It can be seen that for $0 \le b \le 1$ with increase in the value of b the extent of self-focusing increases where as the scenario gets reversed after $b > 1$ i.e., for $b > 1$ with increase in the value of b the extent of self-focusing of the laser.

Figure 3 illustrates the effect of slope of the density ramp on self-focusing of the laser beam. It can be seen that with increase in the slope of density ramp, there is enhancement in the extent of self-focusing of the laser beam. This occurs because with increase in the slope of the density ramp, in the deeper regions of the plasma the laser beam sees lesser index of refraction. Thus, increase in the slope of density ramp enhances the extent of focusing of the laser beam.

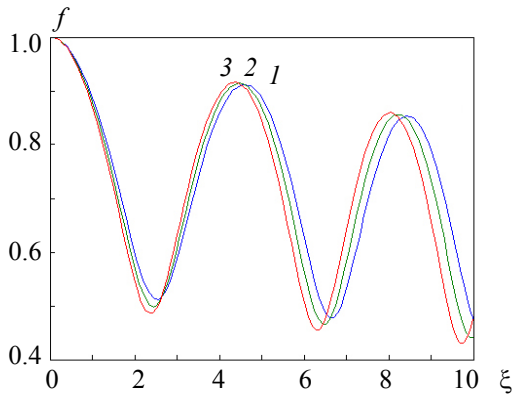

Fig. 3. Effect of the slope of the density ramp on the evolution of the beam width of the laser beam through plasma for a fixed value of the Cosh factor $b = 0.5$, $d' = 0.025$ (*1*), 0.035 (*2*), and 0.045 (*3*),

Excitation of EPW. There are mainly two mechanisms by which laser beams can excite EPWs. The first one is called resonance absorption. As a laser beam penetrates the plasma, much of the energy of its oscillating electric field is given up to surrounding electrons. Near the critical-density surface, however, the natural oscillating frequency of EPW equals the laser frequency. The energy that reaches this depth in the plasma can drive EPWs resonantly to large amplitudes, much as a child on a swing can go progressively higher by pumping in synchrony with the swing's natural motion. The second mechanism for excitation of EPW is three-wave mixing, where an incident laser beam decays into two daughter waves. In general, the mixing is strongest when the amplitudes of the interacting waves are large. The frequency of the pump wave equals the sum of the frequencies of the two daughter waves. Three wave mixing leads to excitation of EPWs by two mechanisms. The first mechanism for the excitation of EPW by three wave mixing is known as two plasmon decay. Here the pump beam splits into two EPWs. The second mechanism for excitation of EPW is called stimulated Raman scattering; here the daughter waves are an EPW and a reflected light wave. In present investigation we have considered resonance absorption as the dominant mechanism for the excitation of EPW. These EPWs are like sound waves in that they propagate as compressions and rarefactions of particles in the direction of wave propagation. An important difference between plasma waves and sound waves is in terms of their dispersion nature. In ordinary gases sound waves are non dispersive i.e., their velocity is independent of wavelength. However, in plasma the EPWs are dispersive in nature. Their speed may increase or decrease as their wavelength shortens, depending on their direction of propagation. Another difference between EPWs and sound waves is that unlike sound waves, EPWs don't affect all the species of the medium-ions essentially remain at rest. The propagation of excited EPW is governed by the wave equation:

$$2ik_{ep}\frac{\partial n_{ep}}{\partial z}=\nabla_{\perp}^{2}n_{ep}+\frac{\omega_{ep}^{2}}{v_{th}^{2}}\left(1+\tan\left(dz\right)\right)\left\{1-\exp\left[-\frac{e^{2}}{8m\omega_{0}^{2}T_{0}K_{0}}E_{0}E_{0}^{\star}\right]\right\}n_{ep}, \tag{13}$$

where, $v_{th}=\sqrt{2KT_0/m}$ is the thermal velocity of plasma electrons. Considering the Gaussian ansatz for the EPW:

$$n_{ep}=\frac{n_{00}}{f_{ep}}\exp\left[-\frac{r}{2r_0^2f_{ep}^2}\right] \tag{14}$$

and using the procedure of above 4 we get the equations for the evolution of beam widths of the EPW

$$\frac{d^2f_{ep}}{d\xi^2}=\frac{1}{f_{ep}^3}-\left(\frac{\omega_{ep}^2r_0^2}{v_{th}^2}\right)\frac{1}{f_{ep}^3}\left(1+\tan\left(d'\xi\right)\right)\left(T_3-bT_4\right), \tag{15}$$

$$T_3=\int_0^{\infty}x^3e^{-x^2}\exp\left[-\frac{f^2}{f_{ep}^2}x\right]\cosh^4\left(bx\right)\exp\left[-\frac{\beta E_{00}^2}{f^2}e^{-x^2}\cosh^2\left(bx\right)\right]dx,$$

$$T_4=\int_0^{\infty}x^2e^{-x^2}\exp\left[-\frac{f^2}{f_{ep}^2}x\right]\cosh^3\left(bx\right)\sinh\left(bx\right)\exp\left[-\frac{\beta E_{00}^2}{f^2}e^{-x^2}\cosh^2\left(bx\right)\right]dx.$$

Equation (15) shows the coupling of EPW with pump beam i.e., ChG laser beam. It can be seen that the density perturbation associated with EPW is very sensitive to the self-focusing of the laser beam. Using Poisson's equation, the electric field of the excited EPW can be obtained:

$$\mathbf{E}_{ep}=E_{ep}\exp\left[i\left(k_{ep}z-\omega_{ep}t\right)\right],$$

$$E_{ep}=\frac{im\omega_{ep}^2}{ck_{ep}f_{ep}}\exp\left[-\frac{r}{2r_0^2f_{ep}^2}\right]. \tag{16}$$

Equation (16) gives the field strength of the excited EPW. The average value of the strength of this field has been obtained by averaging over the cross section of the laser beam. Eqs. (15) and (16) have been solved in association with Eq. (12) by taking $\omega_{ep} = 10^{15}$ rad/s. The corresponding behavior of the field strength of the EPW for different values of Cosh factor and slope of the density ramp has been shown in Figs. 4 and 5. It can be seen that the strength of the electric field of the excited EPW vary in an oscillatory manner with distance of propagation with maximum field occurring at the locations of the focal spots of the laser beam. This is due to the fact that the amplitude of the EPW is very sensitive to the extent of self-focusing of the laser beam. As the pump beam gets self-focused, its intensity increases and consequently the oscillation amplitude of the plasma electrons also increases. This in turn increases the amplitude of EPW. As the beam width of the pump beam evolves in an oscillatory manner, the strength of the excited EPW also shows the similar behavior with maximum field occurring at the location of minimum beam width of the pump.

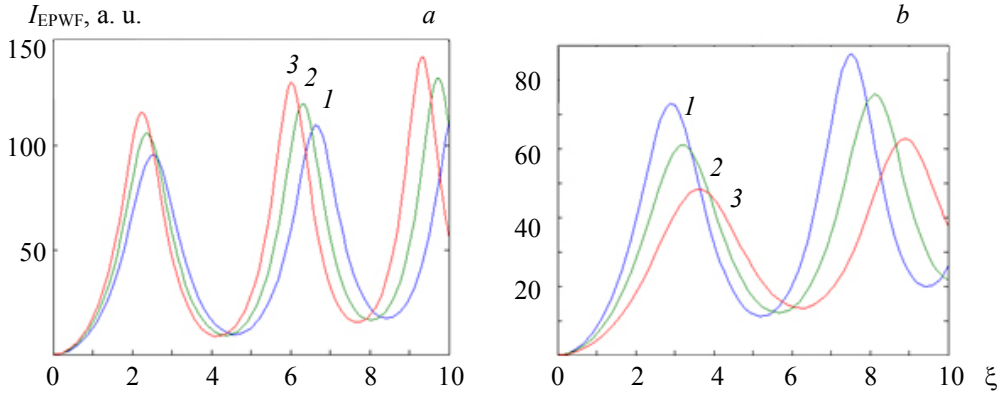

Fig. 4. Effect of the Cosh factor on the evolution of the stimulated Raman reflectivity of plasma for a fixed value of the slope of the density ramp $d' = 0.025$: a) $b = 0$ (*1*), 0.5 (*2*), and 1.0 (*3*), b) $b = 1.1$ (*1*), 1.2 (*2*), and 1.3 (*3*).

From the plots in Fig. 4 it can be seen that the field strength of EPW increases with increase in the value of Cosh factor for $0 \le b \le 1$ and it again starts decreasing with increase in the value of Cosh factor for $b > 1$. This is due to one to one correspondence between the extent of self-focusing of the laser beam and the strength of excited EPW. As the self-focusing of the laser beam increases/decreases with increase in the value of Cosh factor for $(0 \le b \le 1)/(b > 1)$, respectively, there is corresponding increase/decrease in the strength of excited EPW with increase in the value of Cosh factor.

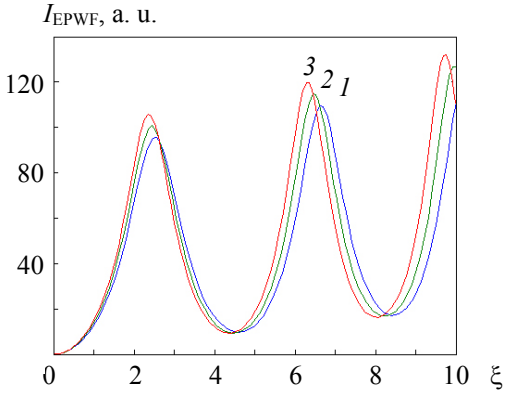

Fig. 5. Effect of the slope of the density ramp on the stimulated Raman reflectivity of plasma for a fixed value of the Cosh factor $b = 0.5$; $d' = 0.025$ (*1*), 0.035 (*2*), and 0.045 (*3*).

Figure 5 depicts the effect of slope of the density ramp on power of excited EPW. It can be seen that the strength of excited EPW increases with increase in the slope of the density ramp. The reason behind this is twofold. With increase in the slope of density ramp the number of electrons contributing to density perturbation associated with EPW increases. With increase in slope of density ramp the extent of self-focusing of laser beam increases. Thus, with increase in slope of the density ramp the strength of excited EPW increases.

Conclusions. We have investigated the excitation of electron plasma wave by an intense ChG laser beam propagating through plasma with density ramp. From the results of present investigation in can be concluded that irradiance profile of the laser beam plays a significant effect on the its propagation characteristics through plasma that further affects the power of excited electron plasma wave. As the irradiance profile converges towards the Gaussian profile the power of excited electron plasma wave significantly gets reduced. The results of present investigation may serve as a guide for the experimentalists working in the area of laser plasma interactions.

REFERENCES

1. R. S. Craxton, K. S. Anderson, T. R. Boehly, V. N. Goncharov, D. R. Harding, J. P. Knauer, R. L. McCrory, P. W. McKenty, D. D. Meyerhofer, J. F. Myatt, A. J. Schmitt, J. D. Sethian, R. W. Short, S. Skupsky, W. Theobald, W. L. Kruer, K. Tanaka, R. Betti, T. J. B. Collins, J. A. Delettrez, S. X. Hu, J. A. Marozas, A. V. Maximov, D. T. Michel, P. B. Radha, S. P. Regan, T. C. Sangster, W. Seka, A. A. Solodov, J. M. Soures, C. Stoeckl, J. D. Zuegel, *Phys. Plasmas*, **22**, 110501 (2015).
2. R. Betti, O. A. Hurricane, *Nature Phys*., **12**, 435 (2016).
3. J. Nuckolls, L. Wood, A. Thiessen, G. Zimmerman, *Nature*, **239**, 139 (1972).
4. E. Gschwendtner, P. Muggli, *Nat. Rev. Phys*., **1**, 246 (2019).
5. E. Esarey, C. B. Schroeder, W. Leemans, *Rev. Mod. Phys*., **81**, 1229 (2009).
6. A. Reagan, M. Berrill, K. A. Wernsing, C. Baumgarten, M. Woolston, J. J. Rocca, *Phys. Rev. A*, **89**, 053820 (2014).
7. N. Lemos, P. King, J. L. Shaw, A. L. Milder, K. A. Marsh, A. Pak, B. B. Pollock, C. Goyon, W. Schumaker, A. M. Saunders, D. Papp, R. Polanek, J. E. Ralph, J. Park, R. Tommasini, G. J. Williams, Hui Chen, F. V. Hartemann, S. Q. Wu, S. H. Glenzer, B. M. Hegelich, J. Moody, P. Michel, C. Joshi, F. Albert, *Phys. Plasmas*, **26**, 083110 (2019).
8. M. Kumar, V. K. Tripathi, Y. U. Jeong, *Phys. Plasmas*, **22**, 063016 (2015).

9. C. Joshi, *Phys. Scr*., **30**, 94 (1990).
10. Q. Feng, L. Cao, Z. Liu, C. Zheng, X. He, *Sci. Rep*., **10**, 3492 (2020).
11. N. Gupta, *J. Opt. Quant. Electron*., **53**, 608 (2021).
12. S. Weber, C. Riconda, V. T. Tikhonchuk, *Phys. Plasmas*, **12**, 043101 (2005).
13. B. J. Albright, L. Yin, K. J. Bowers, B. Bergen, *Phys. Plasmas*, **23**, 032703 (2016).
14. C. J. Randall, J. J. Thomson, K. G. Estabrook, *Phys. Rev. Lett*., **43**, 924 (1979).
15. R. Y. Chiao, C. H. Townes, B. P. Stoicheff, *Phys. Rev. Lett*., **12**, 592 (1964).
16. M. Smid, O. Renner, A. Colaitis, V. T. Tikhonchuk, T. Schlegel, F. B. Rosme, *Nat. Commun.*, **10**, 4212 (2019).
17. R. E. Olson, R. J. Leeper, A. Nobile, J. A. Oertel, G. A. Chandler, K. Cochrane, S. C. Dropinski, S. Evans, S. W. Haan, J. L. Kaae, J. P. Knauer, K. Lash, L. P. Mix, A. Nikroo, G. A. Rochau, G. Rivera, C. Russell, D. Schroen, R. J. Sebring, D. L. Tanner, R. E. Turner, R. J. Wallace, *Phys. Plasmas*, **11**, 2772 (2004).
18. N. V. Kabadi, R. Simpson, P. J. Adrian, A. Bose, J. A. Frenje, M. G. Johnson, B. Lahmann, C. K. Li, C. E. Parker, F. H. Seguin, G. D. Sutcliffe, R. D. Petrasso, S. Atzeni, J. Eriksson, C. Forrest, S. Fess, V. Y. Glebov, R. Janezic, O. M. Mannion, H. G. Rinderknecht, M. J. Rosenberg, C. Stoeckl, G. Kagan, M. Hoppe, R. Luo, M. Schoff, C. Shuldberg, H. W. Sio, J. Sanchez, L. Hopkins, D. Schlossberg, K. Hahn, C. Yeamans, *Phys. Rev. E*, **104**, L013201 (2021).
19. T. S. Gill, R. Kaur, R. Mahajan, *Optik*, **126**, 1683 (2015).
20. T. S. Gill, R. Mahajan, R. Kaur, S. Gupta, *Laser and Part. Beams*, **30**, 509 (2012).
21. N. Gupta, S. Kumar, A. Gnaneshwaran, S. Kumar, S. Choudhry, *J. Opt*., **50**, 701 (2021).
22. A. Singh, N. Gupta, *Phys. Plasmas*, **22**, 062115 (2015).
23. D. Anderson, M. Bonnedal, M. Lisak, *J. Plasma Phys*., **23**, 115–127 (1980).
24. D. Anderson, M. Bonnedal, *Phys. Fluids*, **22**, 105 (1979).